Modeling the Interactions of Congestion Control and Switch Scheduling

Alex Shpiner and Isaac Keslassy
Department of Electrical Engineering
Technion - Israel Institute of Technology
Haifa, 32000, Israel
{shalex@tx, isaac@ee}.technion.ac.il

***Abstract*—In this paper, we study the interactions of user-based congestion control algorithms and router-based switch scheduling algorithms. We show that switch scheduling algorithms that were designed without taking into account these interactions can exhibit a completely different behavior when interacting with feedback-based Internet traffic. Previous papers neglected or mitigated these interactions, and typically found that flow rates reach a fair equilibrium. On the contrary, we show that these interactions can lead to extreme unfairness with temporary flow starvation, as well as to large rate oscillations. For instance, we prove that this is the case for the MWM switch scheduling algorithm, even with a single router output and basic TCP flows. We also show that the iSLIP switch scheduling algorithm achieves fairness among ports, instead of fairness among flows. Finally, we fully characterize the network dynamics for both these switch scheduling algorithms.**

I. Introduction

A. Congestion Control vs. Switch Scheduling

This paper is about combining two conflicting parallel views of the Internet: a *user-centric view*, which considers that user-based end-to-end congestion control algorithms regulate the Internet and that routers are just passive elements of the Internet; and a *router-centric view*, which considers that router-based switch scheduling algorithms regulate the Internet and that users are just passive elements of the Internet.

Both the congestion control and the switch scheduling algorithms have the same common goal: *regulate Internet traffic* so as to maximize link utilization, minimize packet loss, and provide fairness among flows. However, they use quite different means. User-based congestion control algorithms like TCP regulate traffic by decreasing the rates of flows that experience losses, and increasing the rates of flows that do not. On the other hand, router-based switch scheduling algorithms like Maximum Weight Matching (MWM) regulate traffic by providing more services to long backlogged queues, and less services to small queues.

While both traffic regulation algorithms reach high performance when considered independently, we will show that their interacting actions might conflict when put together, and eventually cause more harm than good.

Figure 1 illustrates these issues on a toy model consisting of two flows queued at two different inputs and destined for the same output. Assume that these are TCP flows of rates λ_1 and λ_2, and that the switch implements MWM by always servicing the flow with the longest queue. Independently, both traffic regulation algorithms work fine: if the flows were using TCP but not MWM, e.g. by sharing the same FIFO queue, then they would reach the well-known TCP rate equilibrium [1]–[3]. Likewise, if the two flows were using MWM but not TCP, by using a non-adaptive algorithm with fixed flow rates, then they would both receive 100% throughput as long as $\lambda_1 + \lambda_2 < 1$ [4]–[6].

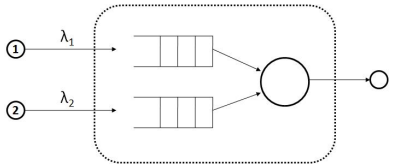

Fig. 1. Simple network of two flows with common output link.

The problem arises when the two traffic regulation algorithms interact. If the queue of the first flow gets larger, MWM will keep servicing it, and therefore the first flow will increase its rate even further in a vicious circle, because TCP will keep receiving ACKs. On the other hand, the second flow will not receive services and get starved. Thus the first flow will overtake all the network resources. The combination of the congestion control and the switch scheduling will cause an *extreme unfairness*, which was absent when they were each alone.

For router designers, this is no trivial result. It might mean that their carefully-designed switch-scheduling algorithms, which work perfectly with all the benchmarks based on non-responsive flows, might break down when introduced in real Internet networks with responsive TCP flows.

For network researchers, this is no trivial result either. It might change the perceived value of many well-known results. For instance, the Birkhoff-von Neumann (BvN) switch scheduling algorithm, which measures the average flow arrival rates and can provide proportional service rates, is known to be fair for non-responsive flows [7]–[9]. In fact, it is one of the only switch scheduling algorithms that are known to provide both throughput and fairness guarantees in practical switch architectures. However, as in the example above, providing more services to a responsive flow might increase its arrival rate in turn, thus increasing its share of the total traffic and leading again to a vicious circle with extreme unfairness. Therefore, it might be that the BvN scheduling algorithm simply does not

fit real Internet traffic, with the vast majority of the bandwidth consisting of TCP responsive flows [10], [11].

These considerations show that congestion control and switch scheduling algorithms *cannot* be designed and analyzed without taking into account their interactions, both in practical router benchmarks and in theoretical network models.

Further, to make things even worse, the example above could also lead to different results, depending on the network topology. For instance, if the queue of the first flow is the longest one and keeps getting serviced, its service rate might exceed its arrival rate, and therefore its size will decrease, until both queue sizes are equal and the second flow gets serviced as well. So it might be that the queue sizes get equalized and stay equal. Or it might also be that the two flows alternately overtake the whole link capacity. Unfortunately, as seen in this paper, *all* these behaviors are possible, and highly depend on network parameters. Therefore, this example also illustrates the inherent *analysis complexity* associated to the interactions between congestion control and switch scheduling.

B. Related Work

Known models of congestion control algorithms often assume *output-queued switching*, i.e. the existence of a single passive queue shared by all the flows destined to a switch-output bottleneck link. For instance, these models have dealt with flow rate equilibria [1]–[3], router buffer sizing [12], [14], [16], [17], TCP dynamics [13], [18], TCP fairness [2], [3], [23], Weighted Fair Queueing (WFQ) [19], and Active Queue Management (AQM) analysis [20], [21]. Unfortunately, output-queued switching cannot be implemented in high-speed routers because of its required memory speedup [22]. Therefore, we will analyze the more realistic input-queued routers and their associated switch scheduling algorithms.

Known models of switch scheduling algorithms often assume *non-responsive traffic* to analyze algorithms like MWM [4]–[6], BvN [7]–[9], and the heuristic iSLIP [24], [25]. These models attempt to achieve more realistic conditions by using admissible non-responsive flows with either variable-size packets [26]–[28], fixed traces [29], router measurements [30], or networked switches [31], [32]. But most of Internet traffic is actually responsive. In this paper, we also consider responsive flows such as TCP flows.

Recently, research works have started modeling the interactions of responsive flows with switch scheduling algorithms. First, [33], [34] model the interaction of TCP sources and the MWM scheduling algorithm. Their model relies on the RED AQM scheme, and they convincingly prove that there always exists a fair system equilibrium point. However, RED mitigates the effects of MWM in that it discriminates against longer queues, while MWM favors them. As a consequence, this model does not reflect the possible extreme unfairness and large rate oscillations that can occur without AQM.

In addition, [35], [36] measure packet delays in a real router fed with a closed-loop ns2-generated TCP traffic. Such an approach can accurately reflect delays at real Internet routers. However, it is dependent on the router implementation, and cannot model arbitrary switch scheduling algorithms.

Further, [37], [38] model the interactions of responsive flows with switch scheduling algorithms in wireless networks. However, they assume congestion control policies that are fundamentally different from TCP.

C. Contributions

In this paper, we attempt to provide a first characterization of the interactions between congestion control and switch scheduling algorithms, using mostly TCP flows and droptail queues. We compare the performances of an output-queued switch; an input-queued switch implementing iSLIP, the scheduling algorithm on which the Cisco 12000 GSR router is based [24]; and an input-queued switch implementing MWM.

By restricting our model to the tractable single-port case, we characterize the system equilibria when they exist, and compare their fairness properties. For instance, we show that output-queued switches are *fair for flows*, while iSLIP-based input-queued switches are *fair for ports*. We also characterize the cases in which MWM leads to *extreme unfairness* with temporary flow starvation.

Further, we discover three different modes of MWM: *starvation, oscillation and equalization*. We find that these modes have fundamentally different properties, and highly depend on the topology parameters.

Last, we completely describe the *network dynamics* for both the iSLIP and MWM scheduling algorithms, using a set of differential equations. We show that iSLIP can be modeled by considering each (input, output) queue as a full output-queued switch. We also find that the behavior of MWM is based on synchronized congestion cycles.

The rest of the work is organized as follows. After defining our model in Section II, we successively analyze the fairness of OQ, iSLIP-based IQ and MWM-based IQ switches under TCP traffic in Sections III, IV and V. Then, we characterize the network dynamics of iSLIP and MWM in Section VI. We finally show simulation results for these models in Section VII.

II. Model and Notations

We now introduce and define our model and notations. We first describe the general network topology and the congestion control of each flow, and then focus on the switch and on its scheduling algorithm.

A. Network Model

Figures 2 and 3 illustrate the general network topology, using a central switch that can be either output-queued or input-queued.

Network — The network includes N groups of flow sources. Each group $1 \leq i \leq N$ consists of m_i persistent TCP-Reno sources and several UDP (or more generally non-responsive) sources modeled as a single UDP Poisson source. All these flow sources are connected to a group aggregation switch, which is connected with its own link of capacity C_{in} to input port i of the $N \times N$ switch. The switch is then connected to the flow destinations with links of capacity C_{out}. Therefore, packets sent by the sources are routed through the group aggregation

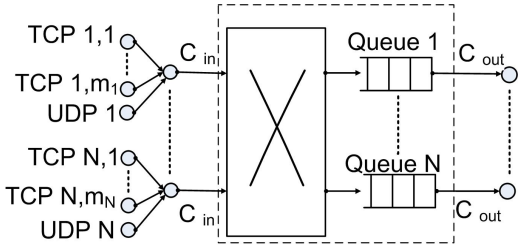

Fig. 2. Network topology based on an output-queued switch.

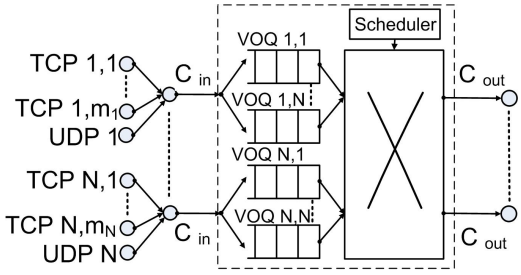

Fig. 3. Network topology based on an input-queued switch.

switch to the main switch, and then to their destination. Acknowledgements (ACKs) come back in the same way. We now make a few simplifying assumptions on the network properties to make the problem more tractable. First, we assume that for these flows, the only bottleneck links are the forwarding links from the switch to the flow destinations.

Assumption 1: The only queues in the network are the packet queues in the switch. In particular, all link capacities but C_{out} are assumed to be infinite, and the backward propagation times are assumed to be fixed.

Round Trip Time —There are $m = \sum_{i=1}^{N} m_i$ TCP flows. For each TCP flow k, let $(w^k(t), Q^k(t), C^k(t))$ respectively denote the congestion window size, number of queued packets, and switch service rate of flow k at time t. Also, let $RTT^k(t)$ and τ^k denote its total (respectively propagation) round-trip time (RTT), i.e. the total time from source to destination and backwards with (without) counting queueing time.

In this paper, we will neglect sub-RTT variations of time-dependent rates, in order to avoid intractable delayed non-linear differential equations. For instance, if $Q^k(t)$ packets of flow k are currently queued and they are currently serviced at rate $C^k(t)$, then we assume that an entering packet from flow k will stay in the queue for $Q^k(t)/C^k(t)$ time-slots. Therefore, the total round-trip time is

$$RTT^k(t) = \tau^k + \frac{Q^k(t)}{C^k(t)} \tag{1}$$

Further, for each input i and output j, let $\mathcal{S}_{ij}$ be the set of TCP flows going through input i and output j. Then, for simplicity, we will assume that all flows in $\mathcal{S}_{ij}$ have the same propagation time.

Assumption 2: The propagation RTT of all flows $k \in \mathcal{S}_{ij}$ is equal and denoted $\tau_{ij}(t) \stackrel{\triangle}{=} \tau^k(t)$.

We now want to characterize the number of packets of each flow in the network. We first make a simplifying assumption to avoid distinguishing between services and departures.

Assumption 3: The service rate $C^k(t)$ of flow k always equals its departure rate, i.e. if $C^k(t) > 0$ then there are always packets from flow k to service in the queue, so $Q^k(t) > 0$.

Window — The total congestion window size $W_{ij}(t)$ of TCP flows in $\mathcal{S}_{ij}$ is denoted $W_{ij}(t) \stackrel{\triangle}{=} \sum_{k\in S_{ij}} w^k(t)$. Let $\tilde{w}^k(t)$ denote the number of packets in the network from flow k at time t, including ACKs. Then, since packets depart from the queue at rate $C^k(t)$ and take a round-trip propagation time of τ^k to come back, there are $C^k(t) \cdot \tau^k$ packets on the links, in addition to the $Q^k(t)$ packets in the queue, hence

$$\tilde{w}^k(t) = C^k(t) \cdot \tau^k + Q^k(t) \tag{2}$$

Moreover, by definition of the congestion window, assuming that TCP does not use the delayed-ACKs feature, we can model [12]

$$w^k(t) \approx \tilde{w}^k(t), \tag{3}$$

which is usually accurate unless flow k just experienced a congestion, in which case $w^k(t)$ falls faster than $\tilde{w}^k(t)$.

B. Switch Model

We now define the notations used for the switch arrivals, schedules, and services.

Arrivals — For each (input, output) pair (i, j), we denote $\lambda_{ij}(t)$ the total rate of packets arriving at input i and destined for output j. We decompose this arrival traffic into two types:

- *TCP traffic*, with arrival rate $\lambda_{ij}^k(t)$ for each flow $k \in \mathcal{S}_{ij}$, yielding a total arrival rate $\lambda_{ij}^{TCP}(t)$; and
- *Poisson UDP traffic*, with fixed total arrival rate λ_{ij}^{UDP}.

Thus, we have: $\lambda_{ij}(t) = \lambda_{ij}^{TCP}(t) + \lambda_{ij}^{UDP} = \sum_{k\in\mathcal{S}_{ij}} \lambda_{ij}^k(t) + \lambda_{ij}^{UDP}$.

Queues — We will assume that time is slotted, and that all data packets have a fixed size, such that each switch output can serve exactly one packet per time-slot.

Let $Q_{ij}(t)$ denote the number of packets arrived at input i, destined to output j, and queued in the switch at time t. We will respectively denote the number of queued TCP and UDP packets as $Q_{ij}^{TCP}(t)$ and $Q_{ij}^{UDP}(t)$. We saw that the number of queued packets from flow $k \in \mathcal{S}_{ij}$ is $Q^k(t) \stackrel{\triangle}{=} Q_{ij}^k(t)$. Therefore: $Q_{ij}(t) = Q_{ij}^{TCP}(t) + Q_{ij}^{UDP}(t) = \sum_{k\in\mathcal{S}_{ij}} Q_{ij}^k(t) + Q_{ij}^{UDP}(t)$. Likewise, the number of queued packets arrived at input i (respectively destined to output j) is $Q_{i\cdot}(t) = \sum_{j=1}^{N} Q_{ij}(t)$ (respectively $Q_{\cdot j}(t) = \sum_{i=1}^{N} Q_{ij}(t)$).

Services — We saw that TCP flow $k \in \mathcal{S}_{ij}$ receives a service rate of $C^k(t) \stackrel{\triangle}{=} C_{ij}^k(t)$. Likewise, the total service rate of all flows belonging to the (input, output) pair (i, j) is denoted $C_{ij}(t)$, including $C_{ij}^{TCP}(t)$ for TCP flows and $C_{ij}^{UDP}(t)$ for UDP flows, so that $C_{ij}(t) = C_{ij}^{TCP}(t) + C_{ij}^{UDP}(t) = \sum_{k\in\mathcal{S}_{ij}} C_{ij}^k(t) + C_{ij}^{UDP}(t)$.

C. Switch Architecture

We will distinguish two types of switches. First, an $N \times N$ *output-queued (OQ)* switch (Figure 2) contains N queues, located at the output ports of the switch. As packets arrive, they are transferred immediately to their corresponding output queue j of length $Q_{\cdot j}(t)$.

An $N \times N$ *input-queued (IQ)* switch (Figure 3) is built using N buffers, located at the input ports of the switch. Each input buffer i is shared dynamically between N *virtual output queues (VOQs)*, which correspond to the N outputs and have total length $Q_{i\cdot}(t)$. When a packet arrives at input i and is destined to output j, it is stored in the corresponding VOQ, denoted VOQ_{ij}, of length $Q_{ij}(t)$.

In an IQ switch, after packet arrivals, a centralized switch scheduler decides on a match between the N input ports and the N output ports, so that no input (resp. output) is matched to more than one output (resp. input). Then, the scheduler picks the head-of-line packets of the selected VOQs to depart according to this match. The scheduler can follow any switch scheduling algorithm in order to decide which packet to serve. Scheduling algorithms considered in this paper include:

- *iSLIP*, a round-robin-based algorithm [24], [25]. In iSLIP, each input (output) keeps a pointer to its preferred output (input), which rotates in a round-robin order once it is matched. Using an iterative process, the scheduler attempts to find a match by giving preference to the inputs and outputs indicated in the pointers. Note that iSLIP reduces to a simple *round-robin (RR)* scheduler on a vector of N VOQs, e.g. when there is only one input or output with active flows.
- *Maximum Weight Matching (MWM)*, which maximizes the weight of the match, with weights given by the queue lengths [4]–[6]. Intuitively, MWM favors larger VOQs. Note that MWM reduces to the *Longest Queue First (LQF)* policy on a vector of N VOQs.

In both switch architectures, the total buffer size at the switch is NB, i.e. B per output in the OQ switch and B per input in IQ switch. Further, all buffers implement a *droptail* policy, i.e. an arriving packet is dropped iff its buffer is full. We will define the set of congestion times for flow k by $\mathcal{T}^k$, where $t \in \mathcal{T}^k$ iff the size Q of the queue that contains flow k satisfies $Q(t^-) < B$ and $Q(t) = B$.

D. Single-Port Model

To get a better grasp of the problem, we will introduce and consider the single output-port model, in which a single output has active flows. Thus, the switch reduces to an $N \times 1$ switch, with simpler notations and switch scheduling algorithms. In this case, we will simplify notations by defining $\lambda_i \stackrel{\triangle}{=} \lambda_{i,1}$, $Q_i \stackrel{\triangle}{=} Q_{i,1}$, and so on. Further, as mentioned above, the iSLIP and MWM switch scheduling algorithms respectively reduce to the round-robin and LQF algorithms.

III. Fairness of OQ switches

In the next sections, we want to compare OQ and IQ switches from the point of view of fairness. To do so, we first define two simple fairness measures: Jain's fairness and utility-based TCP fairness. Then, when considering the single-output case, we show that OQ switches are *fair*.

A. Fairness Measures

Our objective is to analyze the fairness of OQ and IQ switches, i.e. the way in which the available output link capacity is divided between flows. We first define two fairness measures, and then apply these measures to compare the performance of the switches. First, we define *Jain's fairness index* [39]:

Definition 1 (Jain's Fairness): Jain's fairness index for m flows is

$$F \stackrel{\triangle}{=} \frac{\left(\sum_{i=1}^{m} C_i\right)^2}{m \cdot \sum_{i=1}^{m} C_i^2} \tag{4}$$

Next, we define the *utility function* of each TCP flow k, and the resulting *TCP-fair resource allocation.*

Definition 2 (TCP-Fair Resource Allocation): The utility function of a TCP flow k is

$$U_k(C^k) \stackrel{\triangle}{=} -\frac{2}{(RTT^k)^2} \cdot \frac{1}{C^k} \tag{5}$$

Let $\mathcal{S}_{\cdot j}$ be the set of flows k that share output link j of capacity C_{out}. Then a TCP-fair resource allocation is a resource allocation that achieves

$$\begin{aligned} \max \quad & \sum_k U_k(C^k) \\ \text{s.t.} \quad & \sum_{k \in \mathcal{S}_{\cdot j}} C^k \le C_{out} \quad \forall j \\ & C^k \ge 0 \quad \forall k. \end{aligned} \tag{6}$$

Since we assume a FIFO droptail queueing policy, it is hard to analyze the precise behavior of each flow. Therefore, we make a simplifying assumption on flows sharing the same queue.

Assumption 4: Two flows sharing the same queue have equal dropping probabilities. Further, their service rates are proportional to their queue sizes.

B. Fairness analysis

We will now analyze the fairness measure of OQ switches, and later compare it with IQ switches. For simplicity, we consider the *single output-port case*, in which all flows are switched to the same output port j. In this fairness analysis, we assume that all round-trip times are equal, and that there is no UDP traffic. We rely on the following approximation of the steady-state throughput of a TCP flow k with round-trip time RTT^k [2]:

$$C^k = \frac{\sqrt{2}}{RTT^k \cdot \sqrt{d^k}} \tag{7}$$

where C^k and d^k are the steady-state average values of the capacity $C^k(t)$ and the dropping rate $d^k(t)$. We neglect the difference between the average over time and the average seen by packet arrivals. The next theorem shows that the throughput of all flows in the output-queued switch is divided equally at the output link.

Theorem 1 (OQ Switch Throughput): In the OQ switch defined above, the throughput of flow k is:

$$C^k = \frac{C_{out}}{\sum_{i=1}^{N} m_i} \tag{8}$$

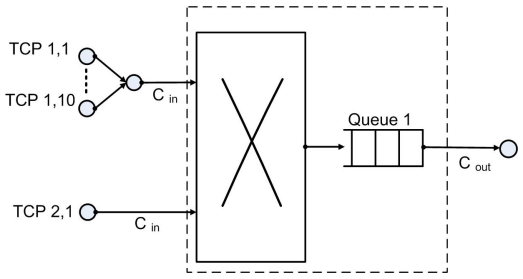

Fig. 4. 2×1 switch example

Proof: By Assumption 4, all flows have the same dropping probability. Therefore, using the steady-state throughput of a TCP flow, as defined in Equation (7), all flows have the same throughput. Finally, by Assumption 3, we have $\sum C^k = C_{out}$, hence the result. ∎

Example 1: As illustrated in Figure 4, consider a 2×1 OQ switch with 10 flows in the first input ($m_1 = 10$) and a single flow in the second input ($m_2 = 1$). Then, the service rate of each flow is

$$C^k = \frac{C_{out}}{m_1 + m_2} = \frac{C_{out}}{11}, \tag{9}$$

independently of its input.

Theorem 2: The OQ switch *maximizes all fairness measures*:
(i) Jain's fairness index achieves its maximum $F = 1$, and
(ii) The total utility function achieves its maximum as well, therefore the resource allocation is TCP-fair.

Proof: Since all flows share the total throughput equally, Jain's fairness is clearly equal to 1: if $m = \sum_{i=1}^{N} m_i$, then

$$F = \frac{\left(m \cdot \frac{C_{out}}{m}\right)^2}{m \cdot m \cdot \left(\frac{C_{out}}{m}\right)^2} = 1. \tag{10}$$

Further, since the total utility function is defined as a sum of equal concave functions of C^k with a single constraint on their sum, the symmetric maximal resource allocation necessarily achieves the maximum total utility function (as also seen using Jensen's inequality, Lagrange duality, or simple matroid optimization). Denote $\alpha = 2/(RTT^k)^2$. Then the total utility function is

$$\sum_{k=1}^{m} U_k(C^k) = m \cdot \left(\frac{-\alpha}{C_{out}/m}\right) = \frac{-\alpha m^2}{C_{out}} \tag{11}$$

∎

IV. Fairness of IQ Switches with iSLIP Scheduling

We saw above that OQ switches are fair. We now want to analyze iSLIP-based IQ switches. We prove that IQ switches using iSLIP scheduling are *unfair* in the general case, and show that they provide *port-fairness* instead of *flow-fairness*.

In order to analyze the fairness of iSLIP-based IQ switches, we assume the same setting as in the analysis of OQ fairness, with a single output-port. In such a setting, the iSLIP algorithm reduces to a simple round-robin (RR) scheduling scheme. In the next theorem, we show that each input i receives an equal share of the output capacity, divided equally among its $m_i > 0$ flows.

Theorem 3 (iSLIP Throughput): In an IQ switch with iSLIP scheduling, the throughput of flow k in input i is

$$C_i^k = \frac{C_{out}}{N \cdot m_i} \tag{12}$$

Proof: The round-robin algorithm provides the same share of the output link capacity to each input. By Assumption 3, this provided service rate also corresponds to departures, and therefore all input ports have the same total departure rate and the round-robin schedule does not need to skip queues in this model. Thus, each input port behaves as an OQ switch of rate C_{out}/N with m_i flows sharing the queue. The result follows from Theorem 1 on the OQ switch throughput. ∎

Example 2: Consider again the network from Example 1, as illustrated in Figure 4, this time with an IQ switch using an iSLIP scheduler. Then, the service rate of each flow in the first input port is $C^k = C_{out}/20$, and the service rate of the flow in the second input port is $C^k = C_{out}/2$. This is clearly an *unfair* allocation among flows.

Based on the Cauchy-Schwarz inequalities, the following theorem shows that iSLIP is unfair under both fairness measures.

Theorem 4: The iSLIP-based IQ switch is *unfair* by both fairness criteria, unless all inputs have the same number of flows. Further,
(i) its Jain's fairness index is

$$F = \frac{N^2}{\left(\sum_{i=1}^{N} m_i\right) \cdot \left(\sum_{i=1}^{N} \frac{1}{m_i}\right)}, \tag{13}$$

(ii) and its total utility function is

$$\sum_k U_k(C^k) = \frac{-\alpha N}{C_{out}} \sum_{i=1}^{N} m_i^2. \tag{14}$$

Proof: The proof is presented in Appendix A. Both fairness measures are shown to be unfair using different Cauchy-Schwarz inequalities, with equality iff all the m_i are equal. ∎

The throughput allocation in an IQ switch using iSLIP is unfair when all ports do not have the same number of flows. More generally, the results above show that the OQ switch maintains fairness *among flows*, while the iSLIP-based IQ switch maintains fairness *among ports*.

V. Fairness of IQ Switches with MWM Scheduling

A. Starvation Mode vs. Oscillation Mode

We now analyze the fairness of IQ switches with MWM scheduling. For simplicity, we want to analyze the 2×1 case mentioned in the Introduction and shown in Figure 1. In such a case, the MWM algorithm is reduced to a simple LQF algorithm. We first neglect timeouts and UDP traffic, and later take them into account.

There are two conflicting intuitions on the expected results in the 2×1 case. First, we might believe that once a queue becomes large, the MWM scheduler keeps servicing it, and so its congestion window will keep growing until the flow takes

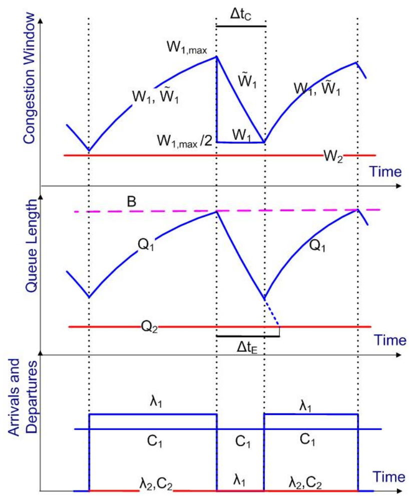

Fig. 5. Starvation mode for two TCP flows in a 2×1 MWM switch

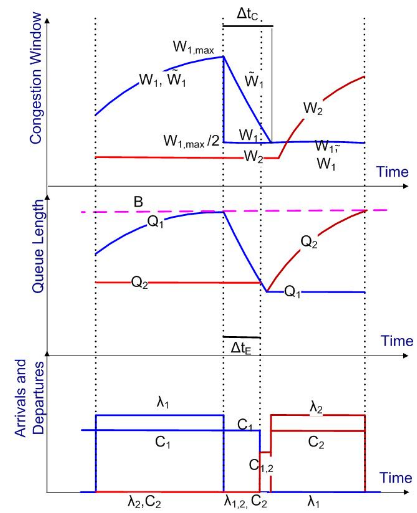

Fig. 6. Oscillation mode for two TCP flows in a 2×1 MWM switch

control over the whole service rate and causes other flows to temporarily starve. So the MWM scheduler might be extremely *unfair* in such a *starvation mode*.

On the other hand, if a flow has the largest queue and keeps getting serviced, its queue can empty out faster, and then another flow will in turn have a larger queue and get service, thus overcoming the first flow. The service rate of each flow will oscillate between 0 and the full capacity C_{out}. So over a long average, the MWM scheduler might actually be somehow more *fair* in this *oscillation mode*.

The following analysis shows that both intuitions can be correct, and both the *starvation* and the *oscillation modes* can occur, depending on the network parameters. For instance, let's assume that at some time t_0 the first queue is longer than the second one:

$$Q_1(t_0) > Q_2(t_0) \tag{15}$$

Then the *starvation mode* occurs when this strict inequality keeps holding at all times $t \geq t_0$, both in *stable phases* (when queue sizes keep growing) and in *congestion phases* (when queue sizes fall).

Figure 5 illustrates the typical behavior of the *starvation mode*, in which the first flow keeps prevailing and the second flow is starved. Since we always have $Q_1(t) > Q_2(t)$, the first flow keeps getting serviced at rate $C_1 = C_{out}$. Therefore it keeps increasing its window size, and its corresponding queue arrival, until $Q_1 = B$. This causes a packet drop, and the window size is halved.

There is then a *race condition* between Δt_C, the time before both the window and the queue of the first flow start growing again, and Δt_E, the time it takes to equalize the queues lengths Q_1 and Q_2. As we will prove, when $\Delta t_C < \Delta t_E$, the first queue is always longer than the second one, and therefore the network stays in *starvation mode*. However, if $\Delta t_C > \Delta t_E$, the two queue lengths get equal, and the other flow might start growing faster, thus the network enters an *oscillation mode* as shown in Figure 6.

In other words, during stable phases, a single prevailing queue is always being serviced, and the other queue is starved — but in *starvation mode*, the same queue is always prevailing, while in *oscillation mode*, the identity of the prevailing queue might change during the congestion phase. As stated in the following theorem, the mode depends in fact on the network topology.

Theorem 5: In the MWM-based IQ scheduler described above, assume that $Q_1(t_0) > Q_2(t_0)$ at time t_0. Then the switch is in *starvation mode* with $Q_1(t) > Q_2(t)$ for all $t \geq t_0$ iff the buffer size B satisfies

$$B > C_{out} \cdot \tau_1 + 2Q_2(t_0) \tag{16}$$

Furthermore, if $B \leq C_{out} \cdot \min(\tau_1, \tau_2)$, the switch is always in *oscillation mode*.

Proof: The proof is presented in Appendix C. ■

In particular, if $Q_2(t_0) = 0$, then the condition for the *starvation mode* corresponds to the well-known rule-of-thumb for the buffer size of an OQ switch [12]. With such a buffer size, we guarantee that the buffer of the first flow never goes empty, and therefore that it is always picked by the MWM scheduler.

In addition, both in the *starvation* and the *oscillation modes*, we can quantify the inter-congestion time T_i of the prevailing flow i. This will help us evaluate the fairness of MWM-based IQ switches.

Theorem 6 (Inter-Congestion Time): Both in the *starvation* and the *oscillation modes*, the inter-congestion time T_i of the prevailing flow i is:

$$T_i = \frac{3 \cdot (\tau_i \cdot C_{out} + B)^2}{8 \cdot C_{out}} \tag{17}$$

Proof: The proof is presented in Appendix D. ■

Note that when we assume the existence of timeouts in starvation mode, Q_2 slightly grows at each timeout. However, even through the second queue is serviced from time to time, the fundamental network properties are unchanged and it is still in *starvation mode*, with a negligible service rate for Q_2.

We further discuss the network properties in Appendix B.

B. UDP Flows and Equalization Mode

We now want to analyze the influence of UDP flows on the network. We show that when the UDP flows have a low rate, their influence is negligible and we still have the same *starvation* and *oscillation modes*. However, for a slightly higher UDP flow rate, we prove the apparition of a third mode, the *equalization mode*, which keeps all queue sizes equal.

Assume that $Q_1(t_0) > Q_2(t_0)$ at time t_0. The intuition is that starvation will happen whenever $\frac{dQ_1}{dt}(t_0) > \frac{dQ_2}{dt}(t_0)$, i.e. $Q_1(t_0)$ is longer than $Q_2(t_0)$ and their difference keeps increasing. Otherwise, if $\frac{dQ_1}{dt}(t_0) < \frac{dQ_2}{dt}(t_0)$ and their difference keeps decreasing, queue 2 will exceed queue 1 at some time t_1 (i.e., $Q_2(t_1) > Q_1(t_1)$), and queue 2 will be serviced in turn. Therefore, we may obtain in turn $\frac{dQ_1}{dt}(t_1) > \frac{dQ_2}{dt}(t_1)$, and eventually queue 1 will exceed again queue 2. Thus, no queue will always prevail. Further, if this equalization happens fast, both queue sizes will remain nearly equal.

We first make the following simplifying assumption, and deduce the conditions for this *equalization mode*.

Assumption 5 (Arrivals and departures of UDP packets): We assume that the rate of the UDP packets is sufficiently low relatively to the service rate, so that during congestions the amount of dropped UDP packets is negligible. Therefore $C_{ij}^{UDP}(t) = \lambda_{ij}^{UDP}$.

Theorem 7 (Equalization mode): In the MWM-based IQ scheduler described above, the switch is in *equalization mode* at time t_0 whenever the arrival rate of UDP packets λ^{UDP} is sufficiently large and satisfies

$$\lambda_2^{UDP} > \frac{C_{out}}{Q(t_0) + C_{out} \cdot \tau_1} \text{ and } \lambda_1^{UDP} > \frac{C_{out}}{Q(t_0) + C_{out} \cdot \tau_2}.$$

In particular, if

$$\lambda_2^{UDP} > \frac{C_{out}}{B + C_{out} \cdot \tau_1} \text{ and } \lambda_1^{UDP} > \frac{C_{out}}{B + C_{out} \cdot \tau_2},$$

then the switch is always in *equalization mode*. Further, if UDP traffic is negligible and satisfies

$$\lambda_2^{UDP} < \frac{C_{out}}{B + C_{out} \cdot \tau_1} \text{ and } \lambda_1^{UDP} < \frac{C_{out}}{B + C_{out} \cdot \tau_2},$$

then as previously the switch is either in a finite-time *starvation mode* or in *oscillation mode*.

Proof: The proof is presented in Appendix E. ∎

C. Fairness measures of MWM switch modes

We now analyze the fairness of the *starvation*, *oscillation*, and *equalization modes* in the simple 2×1 switch example shown in Figure 1, where each input queue serves a single flow.

Starvation Mode — In this case one of the queues is always being serviced, while the other is always starved, i.e. $C_1 = C_{out}, C_2 = 0$. We establish the following fairness result showing that the starvation mode is fundamentally unfair.

Theorem 8: In starvation mode,
(i) Jain's fairness index is $F = \frac{1}{2}$,
(ii) The total utility function is $\sum_i U_i(C_i) = -\infty$.

Proof: First, Jain's fairness index is: $F = \frac{C_{out}^2}{2C_{out}^2} = \frac{1}{2}$. Further, the total utility function is $\sum_i U_i(C_i) = -\frac{2}{(RTT_1)^2}\frac{1}{C_1} - \frac{2}{(RTT_2)^2}\frac{1}{C_2}$, with $C_2 = 0$. ∎

Oscillation Mode — Assume that in oscillation mode, the flow prevailing is determined at each congestion in a round-robin manner. Then we obtain:

Theorem 9: Denote $\alpha_i = \tau_i \cdot C_{out} + B$. Then in oscillation mode,
(i) Jain's fairness index is $F = \frac{(\alpha_1^2+\alpha_2^2)^2}{2(\alpha_1^4+\alpha_2^4)}$.
(ii) The total utility function is

$$\sum_i U_i(C_i) = \frac{-2(\alpha_1^2+\alpha_2^2)}{C_{out}}\left(\frac{1}{\alpha_1^2 \cdot RTT_1^2} + \frac{1}{\alpha_2^2 \cdot RTT_2^2}\right) \quad (18)$$

Proof: Using the inter-congestion times from Theorem 6, $C_1 = C_{out}\frac{T_1}{T_1+T_2}$ and $C_2 = C_{out}\frac{T_2}{T_1+T_2}$, and therefore $C_1 = C_{out}\frac{\alpha_1^2}{\alpha_1^2+\alpha_2^2}$ and $C_2 = C_{out}\frac{\alpha_2^2}{\alpha_1^2+\alpha_2^2}$. We conclude by assigning C_1 and C_2 in fairness Equations (4) and (5). ∎

Equalization Mode — We first prove the following lemma, before characterizing fairness in equalization mode.

Lemma 1: In equalization mode, the approximate service rate C_i of queue i is

$$C_i = C_{out}\frac{\tau_j}{\tau_i + \tau_j}, \quad (19)$$

where $i \neq j$.

Proof: In equalization mode, $Q_i = Q_j$. Using $Q_i = W_i - C_i * \tau_i$ and $C_i + C_j = C_{out}$, we get

$$C_i = \frac{W_i - W_j + C_{out} \cdot \tau_j}{\tau_i + \tau_j} \quad (20)$$

Approximating the average value of W_i (and W_j) as the average between its maximum and minimum values, where the minimum equals half the maximum,

$$W_i \approx \frac{W_{i,max} + W_{i,max}/2}{2} = \frac{3(B + C_i\tau_i)}{4} \quad (21)$$

Substituting into the previous equation, we get the result. ∎

Theorem 10: In equalization mode,
(i) Jain's fairness index is $F = \frac{(\tau_1+\tau_2)^2}{2(\tau_1^2+\tau_2^2)}$
(ii) The total utility function is

$$\sum_i U_i(C_i) = -\frac{2(\tau_1+\tau_2)}{C_{out}}\left(\frac{1}{(RTT_1)^2 \cdot \tau_2} + \frac{1}{(RTT_2)^2 \cdot \tau_1}\right)$$

Proof: By assigning C_1 and C_2 from Lemma 1 into Equations (4) and (5). ∎

UDP Mode — The analysis of UDP Mode is in Appendix F.

VI. Network Dynamics using IQ Switches

In the next section we introduce more general models that rely on differential equations to model the network dynamics, while not restricting the number of inputs and the number of flows per input.

A. Model

We consider again the simplified *single-output* switch model. We now want to describe the network dynamics in the cases of the iSLIP and MWM switch scheduling algorithms. To do so, we first use *many small building blocks*, which describe the behaviors of the network components. Then, we connect them in a single set of equations. Finally, we reduce this set of general equations to a *simplified set of equations*, from which all other equations can be deduced. For instance, the simplified set only considers queue sizes and services rates — and once we solve it, we can deduce window sizes, arrival rates, long-term rate averages, fairness measures, etc.

We will see that the simplified set of equations has an interesting structure: it is always a *double set of equations*, reflecting the two sides of the interactions, i.e. both the *congestion control* and the *switch scheduling* algorithms. In fact, there are *two equations per flow*, one corresponding to the congestion control and one to the switch scheduling. In total, there are $2(m+N)$ equations, for the m TCP and N UDP flows. Further, the congestion control equations are different when TCP is in *stable phase* and *congestion phase*, i.e. between drops and during drops.

There is still one step left beyond this double set of equations. We need to determine when a flow has a packet drop and enters congestion. For instance, we previously defined $\mathcal{T}^k$, the set of congestion times for flow k. Likewise, we define the set of congestion times for input i by $\mathcal{T}_i$, where $t \in \mathcal{T}_i$ iff $Q_i(t^-) < B$ and $Q_i(t) = B$. Then if input i experiences congestion, not necessarily all flows going through this input will experience congestion as well — only those that experience packet drops. Further, a flow with more packets has more chance to experience packet drops. Thus, we need a model linking queue congestion and flow congestion. We will simply use the mean-field model from [13], and assume that the probability that flow k of input i experiences congestion given that input i experiences congestion is

$$P(t \in \mathcal{T}^k | t \in \mathcal{T}_i) = 1 - \left(1 - \frac{w^k}{C_i \cdot \tau_i + B + |\mathcal{S}_i|}\right)^{|\mathcal{S}_i|} \quad (22)$$

In the remainder, we first describe the two simplified sets of equations for iSLIP and MWM. Then, we introduce in subsequent lemmas a few interesting building blocks that were used to construct this simplified set of equations. We present the full proofs in Appendix G.

B. Network Dynamics Theorems

First, we present the dynamics of the iSLIP-based network topology. In the next theorem, the switch-scheduling equations are based on the intuition that iSLIP equally divides output capacity among incoming ports, and divides a port capacity among flows proportionally to their number of queued packets (Equation (23)). In addition, the congestion-control equations successively model TCP flows in stable phase, TCP flows in congestion phase, and UDP traffic (Equation (24)).

Theorem 11 (iSLIP Dynamics): The dynamics of Internet traffic going through an iSLIP switch can be modeled using the following set of $2(m+N)$ equations on the $2(m+N)$ flow variables $\{(Q^k(t), C^k(t))_{1\le k\le m}, (Q_i^{UDP}(t), C_i^{UDP}(t))_{1\le i\le N}\}$:
(i) $m+N$ switch scheduling equations:

$$\begin{cases} C^k(t) = \frac{Q^k(t)}{\sum_{k'\in\mathcal{S}_i} Q^{k'}(t)+Q_i^{UDP}(t)} \cdot \frac{C_{out}}{N} & \forall i, k \in \mathcal{S}_i \\ C_i^{UDP}(t) = \frac{Q_i^{UDP}(t)}{\sum_{k'\in\mathcal{S}_i} Q^{k'}(t)+Q_i^{UDP}(t)} \cdot \frac{C_{out}}{N} & \forall i \end{cases} \quad (23)$$

(ii) $m+N$ congestion control equations, reflecting stable phases and congestion phases:

$$\begin{cases} \frac{d}{dt}(Q^k(t) + C^k(t)\tau^k)^2 = 2C^k(t) & \text{if } t \notin \mathcal{T}^k \\ Q^k(t^+) + C^k(t^+)\tau^k = \frac{Q^k(t^-)+C^k(t^-)\tau^k}{2} & \text{if } t \in \mathcal{T}^k \\ \frac{dQ_i^{UDP}}{dt} = \lambda_i^{UDP} - C_i^{UDP}(t) \end{cases} \quad (24)$$

The next theorem presents the dynamics of the MWM-based network topology. The switch-scheduling equations express the full service rate provided to the longest queue by MWM (Equation (26)). As in Theorem 11, the congestion-control equations model TCP and UDP flows (Equation (27)).

Theorem 12 (MWM Dynamics): The dynamics of Internet traffic going through an MWM switch can be modeled using the following set of $2(N+m)$ equations on the $2(N+m)$ input variables $\{(Q^k(t), C^k(t))_{1\le k\le m}, (Q_i^{UDP}(t), C_i^{UDP}(t))_{1\le i\le N}\}$:
(i) $m+N$ switch scheduling equations: let $\mathcal{A}(t)$ denote the set of inputs with the longest queue at time t, i.e.

$$\mathcal{A}(t) = \{i : Q_i = \max_j Q_j\}, \quad (25)$$

then

$$\begin{cases} C_i^k(t) = \frac{\sum_{k'\in\mathcal{S}_i} C^{k'}(t)+C_i^{UDP}(t)}{\sum_{k'\in\mathcal{S}_i} Q^{k'}(t)+Q_i^{UDP}(t)} \cdot Q_i^k(t) \\ C_i^{UDP}(t) = \frac{\sum_{k'\in\mathcal{S}_i} C^{k'}(t)+C_i^{UDP}(t)}{\sum_{k'\in\mathcal{S}_i} Q^{k'}(t)+Q_i^{UDP}(t)} \cdot Q_i^{UDP}(t) \\ \sum_{k\in\mathcal{S}_i} Q_i(t) = \sum_{k\in\mathcal{S}_j} Q_j(t) \quad \text{if} \quad i,j \in \mathcal{A}(t) \\ \frac{d}{dt}\sum_{k\in\mathcal{S}_i} Q_i^k(t) = 0 \quad \text{if} \quad i \notin \mathcal{A}(t) \\ \sum_{k=1}^m C^k + \sum_{i=1}^N \lambda_i^{UDP} = C_{out} \end{cases} \quad (26)$$

where the number of independent equations for each equation line is successively $(m-N, N, |\mathcal{A}(t)|-1, N-|\mathcal{A}(t)|, 1)$, yielding a total of $m+N$.
(ii) $m+N$ congestion control equations, reflecting stable phases and congestion phases:

$$\begin{cases} \frac{d}{dt}(Q^k(t) + C^k(t)\tau^k)^2 = 2C^k(t) & \text{if } t \notin \mathcal{T}^k \\ Q^k(t^+) + C^k(t^+)\tau^k = \frac{Q^k(t^-)+C^k(t^-)\tau^k}{2} & \text{if } t \in \mathcal{T}^k \\ \frac{dQ_i^{UDP}}{dt} = \lambda_i^{UDP} - C_i^{UDP}(t) \end{cases} \quad (27)$$

As mentioned above, the full proofs appear in Appendix G. We also explain there why the model for the $N \times 1$ iSLIP switch is in fact a combination of N independent models of 1×1 switches, i.e. N FIFO queues. Further, in Appendix H, we provide some additional intuition on the related case of a $1 \times N$ switch with a single input port.

We provide below a proof example, in which we demonstrate the congestion control equations in the stable phase.

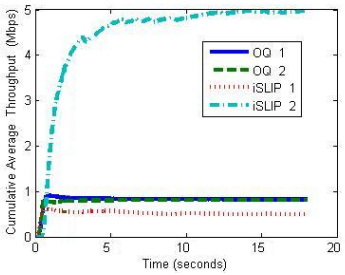

Fig. 7. Simulation of OQ and IQ-iSLIP cumulative average throughput.

Lemma 2: In the *stable phase*, the network satisfies

$$\frac{d}{dt}((Q^k(t)+C^k(t)\tau^k)^2) = 2C^k(t) \tag{28}$$

Proof: First, all flows k in the same input i have the same round-trip time $RTT_i(t) \triangleq RTT^k(t) = \tau^k + \frac{Q^k(t)}{C^k(t)}$, because they have the same $\tau^k(t)$ (Assumption 2) and because their share of the input bandwidth ($C^k(t)$) is proportional to their share of the queue size ($Q^k(t)$) (Assumption 4). Next, in the stable phase, from Equations (2) and (3), the congestion window size of each input i is assumed to satisfy $w^k(t) = C^k(t) \cdot RTT^k(t)$ Further, for each flow k, $\frac{dw^k(t)}{dt} = \frac{1}{RTT^k(t)} = \frac{1}{RTT_i(t)}$, thus $\frac{d}{dt}(Q^k(t)+C^k(t)\tau_i)^2 = \frac{d}{dt}w^k(t)^2 = 2w^k(t) \cdot \frac{d}{dt}w^k(t) = 2\left(C^k(t) \cdot RTT^k(t)\right) \cdot \frac{1}{RTT^k(t)}$, hence the result. ∎

VII. Simulations

A. Simulation Settings

We now want to evaluate the correctness of our models by comparing them with simulation results. We ran ns2 simulations of the network dynamics, and compared them with Matlab implementations of the differential equations in the iSLIP- and MWM-based IQ switch models.

In our simulations, we used default ns2 protocol implementations. For $i, j \geq 0$, we assumed that the round-trip propagation time of flows at input i and output j is $\tau_{ij} = (i+j+1) \cdot \tau_{00}$, with a base propagation time $\tau_{00} = 100$ ms. We also assumed a uniform packet size of 1 KB.

B. Fairness of OQ and IQ-iSLIP Switches

Figure 7 displays simulation results for the 2×1 switch example with 11 flows, as shown in Figure 4 and discussed in Examples 1 and 2. It plots the cumulative average throughput of one flow from each input, assuming both OQ and iSLIP-based IQ. The simulation used $C_{out} = 10$ Mbps, $B = 28$ KB, and a total average rate of UDP flows equal to 1% of the output link capacity C_{out}.

The figure confirms the results presented in the analysis. In the OQ switch, the throughput of different flows equalizes over time even if they are from different inputs, thus resulting in a *fair allocation*. However, in the IQ-iSLIP switch, the throughput of the flow from the second input tends to be ten times larger than the throughput of each of the ten flows from the first input, thus resulting in a *large unfairness*.

C. MWM Modes

Figures 8(a), 8(c) and 8(b) show the evolution of the instantaneous queue lengths of each input in the three MWM modes, assuming the 2×1 switch setting. All these figures were obtained using the same switch architecture, but different network topology conditions (different buffer sizes, propagation times, and output capacity).

Figure 8(a) shows the *starvation mode*, where queue 1 is the prevailing serviced queue and queue 2 is the starved queue. It used a single flow per input, no UDP packets, $C_{out} = 1$ Mbps and $B = 41$ KB.

Figure 8(b) shows the *oscillation mode*, where only one of the queues gets full service rate at each time. In between two full-service states the queue apparently goes through an equalization phase between $t = 565$ seconds and $t = 575$ seconds. As opposed to the *starvation mode*, we can see that the full service is passing from one queue to another. It used five flows per input, no UDP packets, $C_{out} = 5$ Mbps and $B = 150$ KB.

Finally, Figure 8(c) plots the *equalization mode*, in which queue lengths are kept equal. It used a single flow per input, $C_{out} = 2$ Mbps, a total UDP rate of $20\% \cdot C_{out}$, and $B = 31$ KB.

These simulations can be used to validate Theorems 5 and 7. For instance, in the starvation mode settings, the following condition of Theorem 5 holds:

$$\begin{aligned} C_{out} \cdot \tau_1 + 2Q_2(t_0) &\approx 2 \cdot 10^6/8 \cdot 0.1 + 2 \cdot 14 \cdot 10^3/8 \\ &= 40.5\text{KB} < 41\text{KB} = B \end{aligned}$$

D. Switch Dynamics

Figures 9(a) and 9(b) are showing the modeled dynamics and the ns2 simulation results of the 2×1 iSLIP switch with 100 TCP flows per input, using $C_{out} = 100$ Mbps, a total UDP rate of $5\% \cdot C_{out}$, and $B = 180$ KB. On the graphs, $Q_{1,2}$ represents the sizes of each of the queues and $C_{1,2}$ the amount of serviced packets in last 25 ms for each of the queues. We can observe the constant and equal service rate of both queues and the similar graphs of the queue dynamics in the model and in the simulation.

Further, Figures 10(a) and 10(b) compare the MWM switch dynamics in an ns2-based network simulation and in an implementation of the differential-equations model, both being run *under the same topology conditions*. We assumed a 2×1 switch five TCP flows per input, using $C_{out} = 5$ Mbps, a total UDP rate of $5\% \cdot C_{out}$, and $B = 70$ KB.

In both plots, the two queues appear to be in *equalization mode*, with both queue plots barely distinguishable. The queue dynamics seem quite similar in the model and in the simulation, thus providing a partial validation of the model. In particular, there is similarity in the minimal values, maximal values, and slopes of the respective functions.

E. MWM Modes in $N \times N$ Switches

We finally want to evaluate the behavior of MWM in $N \times N$ switches. Such switches are much harder to analyze than $N \times 1$ switches, because of the many interactions between queues. We

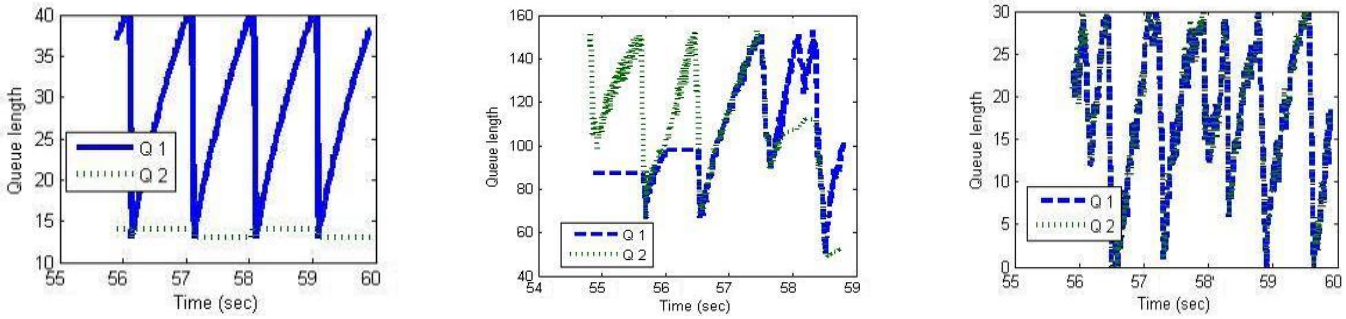

(a) 2×1 MWM – Starvation mode. (b) 2×1 MWM – Oscillation mode. (c) 2×1 MWM – Equalization mode.

Fig. 8. Fairness simulation graphs for all modes.

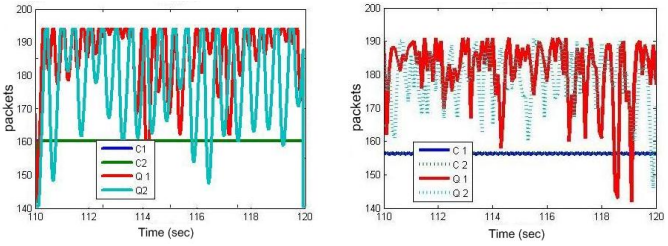

(a) Model. (b) Simulation.

Fig. 9. 2×1 iSLIP switch with 100 TCP flows per input.

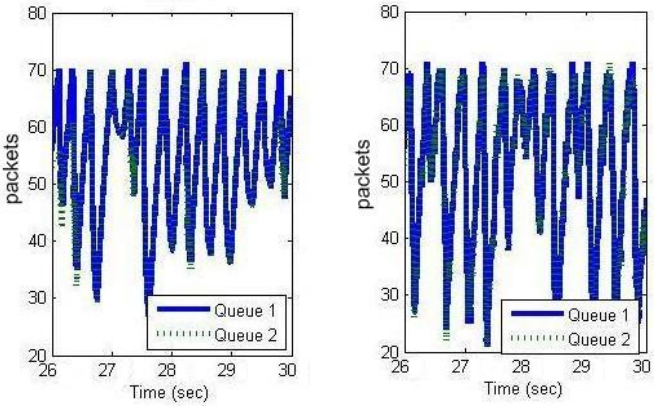

(a) Model. (b) Simulation.

Fig. 10. 2×1 MWM switch dynamics with five TCP flows per input.

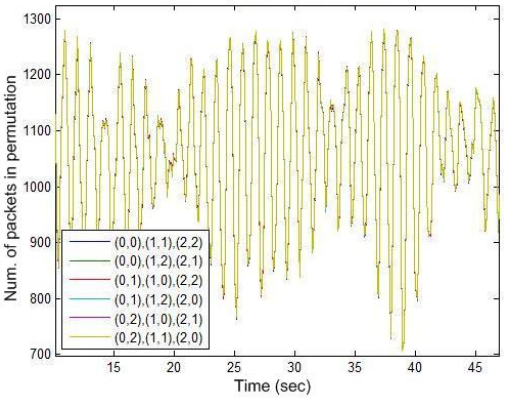

(a) Equalization mode.

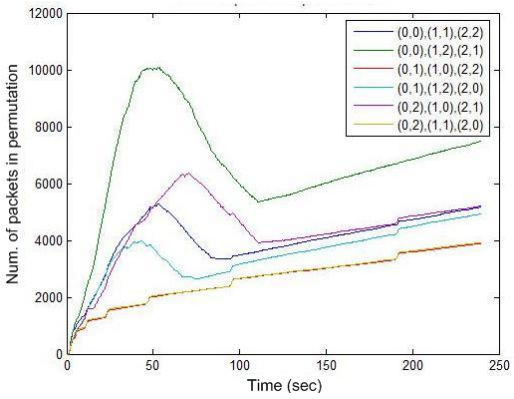

(b) Starvation mode.

Fig. 11. Simulation graphs of 3x3 MWM switch with 100 flows per VOQ.

show below that their observed behavior in simulations reflects the MWM modes analyzed in $N \times 1$ switches.

Figures 11(a) and 11(b) illustrate the behavior of a 3×3 MWM switch under different topology parameters. Both plot the $3! = 6$ possible permutations weights, i.e. the total number of packets in the corresponding VOQs. Both assume 100 flows per (input,output) pair, i.e. a total of 900 flows. Further, Figure 11(a) used $C_{out} = 100$ Mbps, $B = 2.5$ MB, and $\tau_{00} = 100$ ms, while Figure 11(b) used $C_{out} = 10$ Mbps, $B = 10$ MB, and $\tau_{00} = 1$ ms.

We can see that in Figure 11(a), the switch is in *equalization mode*, under which all permutation weights tend to stay equal. On the other hand, in Figure 11(b), the switch is in *starvation mode*, with a single permutation having a weight higher than the others, and therefore always being served. (Note that other permutation weights steadily increase because of UDP and timeout packets that keep arriving.) Therefore, the $N \times N$ switch dynamics reflect the dynamics analyzed in the $N \times 1$ switch; instead of dealing with packets queued in a specific queue, these are now the dynamics of all packets queued in a specific permutation.

VIII. Discussions

Let's now briefly discuss the correctness and generality of the assumptions made in this paper.

Single bottleneck — Assumption 1 presumes a single bottleneck in the network, and therefore neglects the influence of the other queues. This assumption relies on the observation that in the Internet, few flows practically have more than one bottleneck, and they mostly depend on their most congested queue [12]. Thus, this assumption seems realistic enough. However, we also assumed that the congestion only affects packets, not ACKs. This assumption is too restrictive, and ACK congestion is left for future study.

Equal round trip times — Assumption 2 neglects the RTT variations between flows in the same input port. In simulations, we varied the RTTs of different flows, while keeping them ordered by their RTTs to have similar RTTs in each port. We only found an impact of 1–2 % on the resulting flow capacities.

Non-empty queues — Assumption 3 relies on non-empty queues in the iSLIP switch. While this assumption is obviously wrong in the general case, we found that it mostly holds when buffer sizes are large enough. For instance, in our simulations, queue were typically empty less than 1 % of the time.

Drop-tail queues — Assumption 4 presupposes equal dropping probabilities for flows at the same queue. In simulations, we found that this assumption held when averaged over some sufficiently large time period (over 5 seconds), as long as the number of flows was large enough and the loss rate was reasonable.

UDP loss rate — Assumption 5 neglects the number of lost UDP packets compared to the total number of lost packets. We found that it held in simulations as well, as long as the total UDP rate was negligible.

IX. Conclusions

In this paper we modeled the interactions of user-based congestion control algorithms and router-based switch scheduling algorithms. Using single-port switches, we found that these interactions can lead to extreme unfairness and flow starvation, as well as to large rate oscillations. Further, we discovered three modes of MWM behavior, namely the starvation, oscillation and equalization modes. We also modeled the dynamics of both iSLIP and MWM switches, and showed in simulation results that our models were quite close to simulated dynamics.

In this paper, *none* of the studied arbitration modes in IQ switch schemes was found to be fair, further emphasizing the fairness issues resulting from the interactions of congestion control and switch scheduling.

In this paper, we did not exhibit any fair and efficient IQ scheme. Given our assumptions, iSLIP can be seen as less unfair than MWM, because it arbitrates equally across ports and does not discriminate against flows with large RTTs. However, iSLIP does not always provide 100% throughput [24]. Finding a fair scheme that guarantees 100% throughput is not an easy task — we conjecture that it can be reached using credit-based fairness mechanisms, but leave it for future work.

Acknowledgement

This work was partly supported by European Research Council Starting Grant n° 210389.

References

[1] J. Padhye, V. Firoiu, D. Towsley and J. Kurose, "Modeling TCP throughput: a simple model and its empirical validation," *ACM SIGCOMM*, 1998.

[2] F. Kelly, "Mathematical modelling of the Internet," In *Mathematics Unlimited - 2001 and Beyond*, Springer-Verlag, 2001.

[3] R. Srikant, "Models and methods for analyzing Internet congestion control algorithms," In *Advances in Communication Control Networks*, Springer-Verlag, 2004.

[4] L. Tassiulas and A. Ephremides, "Stability properties of constrained queueing systems and scheduling policies for maximum throughput in multihop radio networks, *IEEE Trans. Automatic Control*, vol. 37, no. 12, pp. 1936-1948, Dec. 1992.

[5] N. McKeown, V. Anantharan, and J. Walrand, "Achieving 100% throughput in an input-queued switch," *IEEE Infocom '96*, vol. 1, pp. 296–302, San Francisco, CA, March 1996.

[6] J.G. Dai, B. Prabhakar, "The throughput of data switches with and without speedup," *Proceedings of IEEE INFOCOM*, vol. 2, pp. 556–564, Tel Aviv, Israel, March 2000.

[7] T. T. Lee, and C. H. Lam, "Path switching-a quasi-static routing scheme for large scale ATM packet switches," *IEEE Journal on Selected Areas of Communications*, vol. 15, pp. 914–924, 1997.

[8] T. Weller, and B. Hajek, "Scheduling nonuniform traffic in a packet switching system with small propagation delay," *IEEE/ACM Transactions on Networking*, vol. 5, no. 6, pp. 813–823, 1997.

[9] C. S. Chang, W. J. Chen, and H. Y. Huang, "On service guarantees for input buffered crossbar switches: a capacity decomposition approach by Birkhoff and von Neumann," *IEEE IWQoS'99*, pp. 79–86, London, UK, 1999.

[10] C. Fraleigh *et al.*, "Packet-level traffic measurements from the Sprint IP backbone," *IEEE Network*, vol. 17, pp. 6–16, 2003.

[11] M. Fomenkov *et al.*, "Longitudinal study of Internet traffic in 1998-2003," *WISICT*, vol. 58, pp. 1–6, 2004.

[12] G. Appenzeller, I. Keslassy, and N. McKeown, "Sizing router buffers," *A*CM SIGCOMM, Portland, OR, 2004.

[13] M. Wang, "Mean-field analysis of buffer sizing," *Globecom'07*, Washington DC, Nov. 2007.

[14] D. Wischik and N. McKeown, "Part I: Buffer sizes for core routers," *ACM SIGCOMM Computer Communication Review*, Jul. 2005.

[15] G. Raina, D. Towsley and D. Wischik, "Part II: Control theory for buffer sizing," ACM SIGCOMM Computer Communication Review, Jul. 2005.

[16] R. S. Prasad, C. Dovrolis, and M. Thottan, "Router buffer sizing revisited: the role of the input/service rate ratio," *ACM CoNext*, New York, 2007.

[17] M. Shifrin and I. Keslassy, "Modeling TCP in small-buffer networks," *Networking*, Singapore, May 2008.

[18] R. Shorten, F. Wirth and D. Leith, "Modelling TCP congestion control dynamics in drop-tail environments," *Automatica*, 2007.

[19] H. Hassan, O. Brun, J. M. Garcia, and D. Gauchard, "Integration of streaming and elastic traffic: a fixed point approach," *SIMUTools*, 2008.

[20] T. Bu and D. F. Towsley, "A fixed point approximation of TCP behavior in a network," *ACM Sigmetrics*, 2001.

[21] S. Deb and and R. Srikant, "Rate-based versus queue-based models of congestion control,", *ACM Sigmetrics*, June 2004.

[22] F. Abel *et al.*, "Design issues in next-generation merchant switch fabrics," *IEEE/ACM Transactions on Networking*, vol. 15, no. 6, pp. 1603–1615, 2007.

[23] J. Lee, S. Bohacek, J. P. Hespanha and K. Obraczka, "A study of TCP fairness in high-speed networks," *Technical Report*, USC, July 2005.

[24] N. McKeown, "The iSLIP scheduling algorithm for input-queued switches," *IEEE Transactions on Networking*, vol. 7, no. 2, pp. 188–201, Apr. 1999.

[25] N. McKeown and T. E. Anderson, "A quantitative comparison of scheduling algorithms for input-queued switches," *Computer Networks and ISDN Systems*, 1998.

[26] M. Ajmone Marsan, *et al.*, "Packet-mode scheduling in input-queued cell-based switches," *IEEE/ACM Transactions on Networking*, vol. 10, no. 5, pp. 666–678, Oct. 2002.

[27] Y. Ganjali, A. Keshavarzian, and D. Shah, "Input queued switches: cell switching vs. packet switching," *Infocom '03*, vol. 3, pp. 1651–1658, Mar. 2003.

[28] H. Attiya, D. Hay, and I. Keslassy, "Packet-mode emulation of output-queued switches," *ACM Symposium on Parallelism in Algorithms and Architectures (SPAA '06)*, Cambridge, MA, August 2006.

[29] P. Giaccone, M. Mellia, L. Muscariello, and D. Rossi, "Switches under real internet traffic", *IEEE HPSR*, Phoenix, Arizona, USA, April 2004.

[30] N. Hohn *et al.*, "Bridging router performance and queuing theory," *ACM Sigmetrics*, New York, June 2004.

[31] M. Andrews and L. Zhang, "Achieving stability in networks of input-queued switches," *IEEE/ACM Transactions on Networking*, vol. 11, no. 5, pp. 848–857, 2003.

[32] M. Ajmone Marsan, P. Giaccone, E. Leonardi, and F. Neri, "On the stability of local scheduling policies in networks of packet switches with input queues," *IEEE Journal on Selected Areas in Communications*, vol. 21, no. 4, pp. 642-655, May 2003.

[33] P. Giaccone, E. Leonardi and F. Neri, "On the behavior of optimal scheduling algorithms under TCP sources," *International Zurich Seminar on Communications*, pp. 94–97, Feb. 2006.

[34] P. Giaccone, E. Leonardi and F. Neri, "On the interaction between TCP-like sources and throughput-efficient scheduling policies," *Technical report*, Politecnico di Torino, July 2006.

[35] R. Chertov, S. Fahmy, and N. B. Shroff, "A black-box router profiler," *IEEE Global Internet*, May 2007.

[36] R. Chertov, S. Fahmy, and N. B. Shroff, "A device-independent router model, *Infocom 2008*, Phoenix, Arizona, May 2008.

[37] M.J. Neely, E. Modiano and C.-P. Li "Fairness and optimal stochastic control for heterogeneous networks, *Infocom '05*, pp. 1723–1734, Miami, FL, Mar. 2005.

[38] A. Eryilmaz and R. Srikant, "Fair resource allocation in wireless networks using queue-length-based scheduling and congestion control, *Infocom '05*, pp. 1794–1803, Miami, FL, Mar. 2005.

[39] R. Jain, D. M. Chiu, and W. Hawe, "A quantitative measure of fairness and discrimination for resource allocation in shared systems," *DEC Research Report TR-301*, 1984.

APPENDIX A
PROOF OF THEOREM 4

Proof: Jain's fairness index is:

$$\begin{aligned} F &= \frac{\left(\sum_{i=1}^{N}\sum_{k=1}^{m_i}\frac{C_{out}}{N\cdot m_i}\right)^2}{\left(\sum_{i=1}^{N} m_i\right)\cdot\left(\sum_{i=1}^{N}\sum_{k=1}^{m_i}\left(\frac{C_{out}}{N\cdot m_i}\right)^2\right)} \\ &= \frac{\left(\sum_{i=1}^{N} m_i\cdot\frac{1}{m_i}\right)^2}{\left(\sum_{i=1}^{N} m_i\right)\cdot\left(\sum_{i=1}^{N} m_i\cdot\frac{1}{m_i^2}\right)} \\ &= \frac{N^2}{\left(\sum_{i=1}^{N} m_i\right)\cdot\left(\sum_{i=1}^{N}\frac{1}{m_i}\right)} \end{aligned} \tag{29}$$

By the Cauchy-Schwarz inequality,

$$N^2 = \left(\sum_{i=1}^{N}\sqrt{m_i}\cdot\frac{1}{\sqrt{m_i}}\right)^2 \le \left(\sum_{i=1}^{N} m_i\right)\cdot\left(\sum_{i=1}^{N}\frac{1}{m_i}\right), \tag{30}$$

i.e. $F \le 1$, with equality iff all the m_i are equal. Likewise, denote $\alpha = 2/(RTT^k)^2$. Then the total utility function is

$$\begin{aligned} \sum_k U_k(C^k) &= \sum_{i=1}^{N}\sum_{k=1}^{m_i}\left(-\frac{\alpha}{C^k}\right) \\ &= -\alpha\sum_{i=1}^{N}\sum_{k=1}^{m_i}\frac{N\cdot m_i}{C_{out}} \\ &= \frac{-\alpha N}{C_{out}}\sum_{i=1}^{N} m_i^2 \\ &= \frac{-\alpha}{C_{out}}\left(\sum_{i=1}^{N}1^2\right)\left(\sum_{i=1}^{N} m_i^2\right) \\ &\overset{(a)}{\le} \frac{-\alpha}{C_{out}}\left(\sum_{i=1}^{N}1\cdot m_i\right)^2 \\ &= \frac{-\alpha m^2}{C_{out}}, \end{aligned} \tag{31}$$

where (a) follows from the Cauchy-Schwarz inequality, with equality iff all the m_i are equal. ■

APPENDIX B
STARVED QUEUE LENGTH IN MWM-STARVED MODE

The maximal length of the starved queue is the minimal length of the prevailing queue. Otherwise, it contradicts the existence of starvation.

Proposition 1 (Starved queue length): The length of the starved queue 2 behaves according to

$$\frac{dQ_2(t)}{dt} = \left\lfloor log_2\left(\frac{t}{RTO}+1\right)\right\rfloor \tag{32}$$

where RTO is either the maximum Retransmission Time-Out value or the RTT of the last successful ACK as measured by the source, and

$$Q_{2,max} = Q_{1,min} \tag{33}$$

Proof: Based on the properties of the TCP-Reno retransmission timer. The first retransmission timer expires after the last previous measured RTT or the predefined maximum Retransmission Time-Out value:

$$TO_1 \triangleq RTO = \min(RTT, MAXRTO) \tag{34}$$

Each next retransmission timer is twice longer than the previous one:

$$TO_i = 2\cdot TO_{i-1} \tag{35}$$

So, suppose that at time $t=0$, $Q_2(t)=0$. Then:

$$\begin{aligned} Q_2(t) &= 1 \quad \text{if } RTO \le t < 3\cdot RTO \\ &= 2 \quad \text{if } 3\cdot RTO \le t < 7\cdot RTO \\ &= i \quad \text{if } (2^i-1)\cdot RTO \le t < (2^i)\cdot RTO \end{aligned}$$

i.e.

$$Q_2(t) = i \text{ if } i \le \log\left(\frac{t}{RTO}+1\right) < i+1 \tag{36}$$

So,

$$\frac{dQ_2(t)}{dt} = \left\lfloor log_2\left(\frac{t}{RTO}+1\right)\right\rfloor \tag{37}$$

■

APPENDIX C
PROOF OF THEOREM 5

We prove Theorem 5 by first proving three lemmas on the general dynamics of flow k, and then using them to characterize the needed conditions for the starvation mode.

The first lemma characterizes the dynamics of the window size of flow k. It distinguishes the congestion times $\left(t \in \mathcal{T}^k\right)$ in which the window size is halved, the times that follow congestion in which the window size does not change as long as it's less than the number of packets in the network $\left(\tilde{w}^k(t) \geq w^k(t)\right)$, and the other times in which the growth rate of the window size is $1/RTT^k(t)$.

Lemma 3: The congestion window size $w^k(t)$ of flow k is approximated by:

$$\begin{cases} w^k(t^+) = \frac{w^k(t^-)}{2} & \text{if } t \in \mathcal{T}^k \\ \frac{dw^k(t)}{dt} = 0 & \text{if } \tilde{w}^k(t) > w^k(t), t \notin \mathcal{T}^k \\ \frac{dw^k(t)}{dt} = \frac{1}{RTT^k(t)} & \text{if } \tilde{w}^k(t) \leq w^k(t), t \notin \mathcal{T}^k \end{cases} \quad (38)$$

Proof: These equations are based on the behavior of the TCP-Reno protocol, as explained above. ∎

The next lemma characterizes the arrival rate of flow k.

Lemma 4: The arrival rate $\lambda^k(t)$ of flow k is approximated by

$$\lambda^k(t) = \begin{cases} 0 & \text{if } \tilde{w}^k(t) > w^k(t) \\ \frac{w^k(t)}{RTT^k(t)} & \text{if } \tilde{w}^k(t) \leq w^k(t) \end{cases} \quad (39)$$

Proof: When $\tilde{w}^k(t) > w^k(t)$, just after congestion, the source of flow k stops sending packets, therefore $\lambda^k(t) = 0$, until $\tilde{w}^k(t) \leq w^k(t)$ again. Then, there are $\tilde{w}^k(t) \approx w^k$ packets on the network (Equation (3)) distributed over a total time of RTT^k, so the sending rate is the ratio of these quantities. ∎

The last lemma compares the arrival rate $\lambda^k(t)$ with the service rate $C^k(t)$.

Lemma 5: When $\tilde{w}^k(t) \leq w^k(t)$, the arrival rate $\lambda^k(t)$ of flow k follows

$$\lambda^k(t) = C^k(t) + \frac{1}{RTT^k(t)} - \frac{dC^k(t)}{dt}\tau^k \quad (40)$$

and therefore

$$\frac{dQ^k(t)}{dt} = \frac{1}{RTT^k(t)} - \frac{dC^k(t)}{dt} \cdot \tau^k \quad (41)$$

Proof: We know that $w^k(t) = Q^k(t) + C^k(t) \cdot \tau^k$ from Equations (2) and (3). Therefore, after differentiation and using Lemma 3, we get $\frac{dQ^k}{dt} = \frac{1}{RTT^k(t)} - \frac{dC^k}{dt}\tau^k$. Finally, using $\frac{dQ^k}{dt} = \lambda^k(t) - C^k(t)$ (Assumption 3), we get the result. ∎

We are finally ready to prove Theorem 5.

Proof of Theorem 5: First, let's prove that $Q_1(t) > Q_2(t)$ in the stable phase following t_0 and preceding congestion. Assume by contradiction that this is only the case until time $t_0 + \Delta t$. By the proof of Lemma 5, $\frac{dQ^k}{dt} = \frac{1}{RTT^k(t)} - \frac{dC^k}{dt}\tau^k$. If until $t_0 + \Delta t$ the first flow is serviced at rate C_{out} while the second flow does not receive any service, then the queues keep growing at the same rate, because round-trip times are presumed equal. Therefore $Q_1(t_0 + \Delta t) > Q_2(t_0 + \Delta t)$ and there is contradiction.

Next, let's analyze the congestion phase. By Lemma 3, before congestion at time $T \in \mathcal{T}^k$, the window size w_1 is at its maximum and equal to the maximum number of packets of flow 1 in the network:

$$w_1(T^-) = w_{1,max} = C_{out} \cdot \tau_1 + B. \quad (42)$$

During congestion the window size is halved and $\tilde{w}_1(T^+) \approx w_1(T^-) > w^1(T^+)$. The congestion period ends when $\tilde{w}_1(t) \approx w_1(t)$ again, i.e. once $w_{1,max}/2$ packets have been transmitted at rate C_{out}. Thus the congestion period lasts

$$\Delta t_C = \frac{w_{1,max}/2}{C_{out}} = \frac{B}{2C_{out}} + \frac{\tau_1}{2} \quad (43)$$

Further, the time period needed to equalize queues lengths after congestion is

$$\Delta t_E = \frac{B - Q_2(t_0)}{C_{out}} \quad (44)$$

This is because there are $Q_1(T^-) = B$ packets of flow 1 and $Q_2(T^-) = Q_2(t_0)$ packets of flow 2 before congestion, while Q_1 decreases at rate C_{out} while Q_2 is kept constant. Therefore, to keep $\Delta t_C < \Delta t_E$, we obtain the lower-bound on B stated in the theorem. Q_2 is then kept constant during both the fluid and congestion phases, and therefore the same results can be obtained in the following stages as well. ∎

APPENDIX D
PROOF OF THEOREM 6

Proof of Theorem 6: [12] introduced the following model for the evolution of the congestion window size:

$$w^k(t) = \sqrt{C_{out} \cdot t + (w^k(0))^2}. \quad (45)$$

Assigning $w^k(0) = \frac{w_{max}}{2} = \frac{2C_{out} \cdot \tau + B}{2}$, and $w^k(T) = 2C_{out}\tau + B$, we get the result. ∎

APPENDIX E
PROOF OF THEOREM 7

In order to prove Theorem 7, we first prove the following preliminary lemmas.

Lemma 6: The length of the serviced queue Q_1 is expressed by

$$\begin{aligned} \frac{dQ_1}{dt}(t) &= \lambda_1^{TCP}(t) + \lambda_1^{UDP}(t) - C_1^{TCP}(t) - C_1^{UDP}(t) \\ &= \frac{1}{RTT_1(t)} - \frac{dC_1^{TCP}}{dt}\tau_1 \end{aligned} \quad (46)$$

Proof: Follows from Assumption 5 and Theorem 5. ∎

Lemma 7: The length of the unserved queue 2 is expressed by

$$\frac{dQ_2}{dt}(t) = \lambda_2^{UDP} \quad (47)$$

Proof: For the unserved queue, there is no service so $C_2 = 0$. Because TCP packets are not serviced, they are also not acknowledged, and as a result, no new TCP packets arrive, thus $\lambda_2^{TCP} = 0$ (neglecting timeout packets, as assumed previously). ∎

Proof of Theorem 7: Starvation happens if $\frac{dQ_1}{dt}(t) > \frac{dQ_2}{dt}(t)$ for all t. Combining Equations (46) and (47) and assigning $Q_{1,max} = B$, we get the final result. ∎

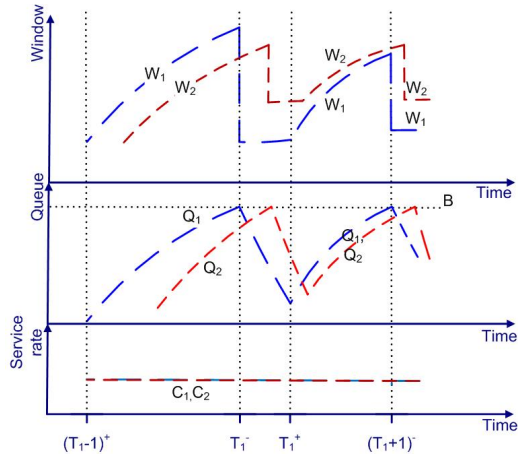

Fig. 12. 2×1 iSLIP model.

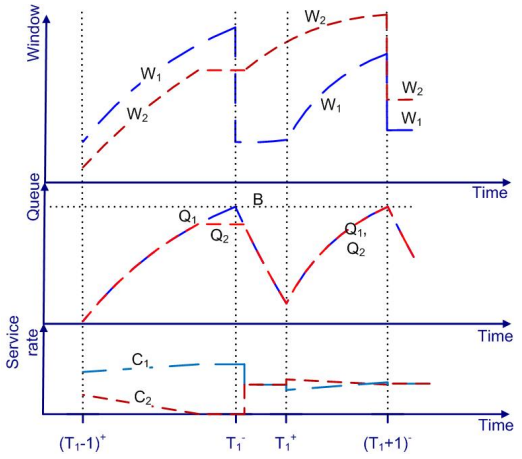

Fig. 13. 2×1 MWM model.

APPENDIX F
FAIRNESS MEASURES OF MWM SWITCHES - UDP MODE

We now analyze the case where traffic only consists of UDP flows, without any TCP flows.

Lemma 8 (UDP Mode Throughput): In a 2×1 MWM switch *with only UDP flows* the approximated service rate C_i of queue i is

$$C_i = \frac{C_{out} + \lambda_i^{UDP} - \lambda_j^{UDP}}{2} \tag{48}$$

where $i \neq j$.

Proof: Assume $\lambda_i^{UDP} > \lambda_j^{UDP}$. The amount $\Delta\lambda_{i,j}^{UDP} = \lambda_i^{UDP} - \lambda_j^{UDP}$ is the first to depart from queue i. The rest $(C_{out} - \Delta\lambda_{1,2}^{UDP})$ is divided equally between the queues:

$$C_i = \Delta\lambda_{1,2}^{UDP} + \frac{C_{out} - \Delta\lambda_{1,2}^{UDP}}{2} \tag{49}$$

C_j is found using $C_j = C_{out} - C_i$. ∎

Theorem 13 (Fairness of UDP Mode): Jain's fairness index is

$$F = \frac{1}{1 + \left(\frac{\lambda_1^{UDP} - \lambda_2^{UDP}}{C_{out}}\right)^2} \tag{50}$$

Proof: By assigning C_1 and C_2 from Lemma 8 into Equation (4). ∎

Note that the total TCP utility function does not apply to this case.

APPENDIX G
NETWORK DYNAMICS: PROOFS OF THEOREMS 11 AND 12

In the proofs below, for each congestion time $T \in \mathcal{T}_i$ we distinguish two different times for simplicity. Let $t = T^-$ be the time when the congestion of the flow happened and $t = T^+$ be the time when the flow recovered form the congestion.

Figures 12 and 13 illustrate the notations and behavior of the dynamics model for iSLIP and for MWM. The model composed of two phases: the *stable phase* and the *congestion phase*.

The *stable phase* models the stable situation, when queues are not full. The output link is fully utilized, the congestion windows are continuously increasing (because there are no drops), so the queues are continuously increasing too (Equations (2) and (3)). During the *stable phase* of queue i, the arrival rate exceeds the service rate, i.e. $\lambda_i \geq C_i$.

The *congestion phase* starts immediately after the congestion indication. Following congestion, there is window halving: the source waits for packets to be acknowledged, in order to equalize the number of packets on the fly to the window size. Meanwhile, the arrival rate decreases, and therefore the queue length decreases as well, because the arrival rate is lower then the service rate. Therefore, during the *congestion phase* of queue i, $\lambda_i < C_i$.

TCP stable phase — We already proved in Lemma 2 the following N equations of the TCP stable phase.

$$\frac{d}{dt}((Q^k(t) + C^k(t) \cdot \tau^k)^2) = 2C^k(t) \tag{51}$$

TCP congestion phase — Next is the set of m equations of the TCP congestion phase.

Lemma 9 (TCP congestion phase equations): In the congestion phase, each TCP flow k satisfies

$$Q^k(T^+) + C^k(T^+) \cdot \tau^k = \frac{Q^k(T^-) + C^k(T^-) \cdot \tau^k}{2} \tag{52}$$

Proof: Resulting immediately from the properties of TCP-Reno and based on the dynamics of w^k that were shown in Lemma 3 (in Appendix C):

$$\begin{aligned} w^k(T^-) &= Q^k(T^-) + C^k(T^-) \cdot \tau^k \\ w^k(T^+) &= \tfrac{w^k(T^-)}{2} \end{aligned} \tag{53}$$

∎

iSLIP switch scheduling — The service rate of queue i in an iSLIP switch is defined by the number of input ports (N), as shown in the following lemma.

Lemma 10 (iSLIP switch equations): The service rate $C_i(t)$ of input queue i in an $N \times 1$ iSLIP switch is defined by the next equation:

$$C_i(t) = \frac{C_{out}}{N} \tag{54}$$

Proof: The service rate of the switch is divided equally between the inputs, as showed in Theorem 3. ∎

Note that the $N \times 1$ iSLIP switch with service rate C_{out} can be modeled as N FIFO queues with service rate C_{out}/N, as each queue receives an equal service rate independently of each other.

MWM switch scheduling — We denote $\mathcal{A}(t)$ as the set of active queues at time t, i.e. queues with $C_i(t) > 0$. Then using MWM, all queues $i, j \in \mathcal{A}(t)$ tend to have equal length: $Q_i(t) = Q_j(t)$ at time t.

Lemma 11 (Queue equalization): If $0 < C_i(t), C_j(t) < C_{out}$, the lengths of the queues i, j behave according to

$$Q_i(t) = Q_j(t) \tag{55}$$

Proof: MWM scheduling gives service to the longest queue. If at some time several queues were serviced, they all have the longest queue length, and therefore can be modeled as equal. ∎

Next is the set of the N equations of the MWM switch scheduling.

Lemma 12 (MWM switch scheduling equations):

$$\begin{cases} Q_i(t) = Q_j(t) & \text{if } \ i, j \in \mathcal{A}(t) \\ dQ_i^{TCP}(t) = 0 & \text{if } \ i \notin \mathcal{A}(t) \\ \sum_{i=1}^{N} C_i = C_{out} \end{cases} \tag{56}$$

Proof: Resulting form Lemma 11 and the TCP-Reno properties. ∎

Per-flow equations — The service rate of each TCP flow satisfies the following lemma.

Lemma 13 (Per-flow equations): Each TCP flow k in input i behaves according to the next set of equations:

$$\begin{cases} C_i^k(t) = C_i(t) \cdot \frac{Q_i^k(t)}{Q_i(t)} \\ \frac{dQ_i^k}{dt} = \lambda_i^k(t) - C_i^k(t) = \frac{dw_i^k}{dt} - \frac{dC_{\tau_i}}{dt} - C_i^k(t) \end{cases} \tag{57}$$

The dynamics of w_i^k are shown in Lemma 3 (in Appendix C).

Proof: The first equation results from Assumption 4, stating that the service rates of two flows sharing the same queue are proportional to their queue sizes. The second equation results from the queue dynamics [12]. ∎

UDP equations — The next set of equations describes the influence of UDP traffic.

Lemma 14 (UDP equations):

$$\begin{cases} Q_i^{UDP} = Q_i - Q_i^{TCP} \\ C_i^{UDP} = C_i - C_i^{TCP} \\ C_i^{UDP} = \frac{Q_i^{UDP}}{Q_i} C_i \\ \frac{dQ_i^{UDP}}{dt} = \lambda_i^{UDP} - C_i^{UDP} \end{cases} \tag{58}$$

Proof: The first two equations result from the definitions of Q_i^{UDP} and C_i^{UDP}. As in Lemma 13, the third equation comes from Assumption 4, stating that the service rates of two flows sharing the same queue are proportional to their queue sizes. The last equation comes from Assumption 3. ∎

APPENDIX H
INTUITION ON THE $1 \times N$ SWITCH

Consider the $1 \times N$ single-port model with a single input and many outputs. In this case the input buffer of size B is shared between all the VOQs of flows destined to different outputs. Therefore, gaining some intuition is much more complex, because of the interactions between all the flows. However, the analysis above helps provide some intuition.

iSLIP — Considering Assumption 3, which basically assumes that queues are never empty, we conclude that a $1 \times N$ iSLIP switch should behave similarly to an $N \times 1$ switch, i.e. each queue should receive C_{out}/N of the bandwidth independently of the other queues, and can be modeled as N FIFO queues with service rate of C_{out}/N.

MWM Starvation and Oscillation Mode— The maximal queue length now depends on the length of other queues because of the queue sharing, therefore the buffer size in condition in Theorem 5 should change from B to $B - Q_2(t_0)$.

MWM Equalization Mode— Because of the queue equalization effect, an $N \times 1$ MWM switch with buffer size B should be similar to a $1 \times N$ MWM switch with buffer size B/N, i.e. the maximal length of each VOQ should be B/N. Theorem 7 is changed accordingly as the buffer size should be B/N instead of B.